IOP Conf. Series: Journal of Physics: Conf. Series **1063** (2018) 012118 doi:10.1088/1742-6596/1063/1/012118

Investigation on strain dependent elastic behavior for accurate springback analysis

S Vitzthum[1*], M Eder[1], C Hartmann[1] and W Volk[1]

Chair of Metal Forming and Casting, Department of Mechanical Engineering, Technical University of Munich, Walther-Meissner-Str. 4, 85748 Garching, Germany

*simon.vitzthum@utg.de

Abstract. In the field of metal forming the effect of springback is of great importance and is one of the research areas. The amount of springback depends substantially on the materials' elastic behavior and the degree of strain hardening. Former studies showed that Young's modulus is influenced by strain hardening and thus detailed knowledge about this correlation is necessary. For an accurate description of strain dependent Young's modulus, a generally valid and consistent formulation in terms of continuum mechanics is required. To reconsider existing formulations, a close examination of the additive decomposition of elastic and plastic strains is necessary that is revealed within this study. Cyclic tensile tests with mild steel DX56 are performed to investigate the strain dependency of Young's modulus experimentally. The theoretically derived formulation is applied to the experimental results. On this basis different determination methods for identifying Young's modulus are utilized and finally analyzed in terms of springback prediction. Finally a new strategy to predict springback is proposed.

1. Introduction

High strength steel is common in vehicle body manufacturing, because of its high yield stress compared to its density [1]. However, the high yield stress to Young's modulus ratio of this steel grades possibly leads to critical geometric deviations caused by springback [2]. Springback occurs after opening the tools of a forming process, because of releasing stored elastic energy. This elastic recovery is one of the challenges in the metal forming industry [3]. The extent of springback is mainly influenced by the elastic-plastic behavior [4]. Hence, many former studies investigated the behavior of elastic recovery showing a dependency between strain hardening and Young's modulus. Morestin and Boivin [5] investigated the variation of Young's modulus with increasing prestrain in cyclic tensile-compression tests for several steel grades. Their results show a decrease of Young's modulus up to 20 % in relation to the work hardening. Findings of Andar et al. [6] reveal similar behavior. Hence, for precise prediction of springback using FE analysis, deep understanding of Young's modulus' strain dependency is mandatory. Cleveland and Ghosh [7] showed in cyclic tensile tests that the elastic unloading behaves nonlinear in contrast to Hooke's law. There are various conjectures and explanations for this nonlinear behavior [7–9]. Depending on the determination method, the nonlinearity influences the value of Young's modulus significantly [10]. A consistent determination of Young's modulus is possible based on suitable strain and stress measures only. Thus, within this study a continuum mechanics based theory for the formulation of Young's modulus is established. Based on results of cyclic tensile tests with mild steel DX56, different methods to determine Young's modulus are used and compared. Furthermore, a data-based method to predict elastic recovery is shown incorporating experimental results of cyclic tensile tests and avoiding an explicit determination of Young's modulus.

2. Theoretical description of elasticity

For the modeling of an elastic-plastic material behavior, a consistent additive decomposition of the total strain into elastic and plastic strain is essential. Therefore, the multiplicative decomposition of the deformation gradient $\boldsymbol{F}$ into elastic and plastic portions is utilized (eq. 1). It is adequate to add an intermediate configuration ${}^{I}\mathcal{B}$ between reference ${}^{0}\mathcal{B}$ and current configuration $\mathcal{B}$, as shown in fig. 1 [11]. A consistent additive decomposition of strains can be shown for the Euler-Almansi strain tensor ${}_{\boldsymbol{A}}\boldsymbol{\varepsilon}$. It acts on the current configuration and is defined as shown in eq. 2.

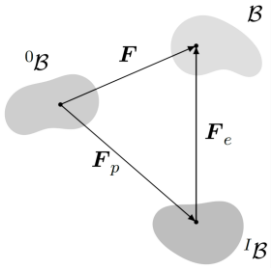

Figure 1. Configurations in elastic-plastic formulation.

$$\boldsymbol{F} = \boldsymbol{F}_e \cdot \boldsymbol{F}_p \tag{1}$$

$${}_{\mathrm{A}}\boldsymbol{\varepsilon} = \frac{1}{2}(\mathbf{1} - \boldsymbol{F}^{-T} \cdot \boldsymbol{F}^{-1}) = \frac{1}{2}(\mathbf{1} - \boldsymbol{V}^{-2}) \tag{2}$$

An elastic pull back of this covariant strain tensor from $\mathcal{B}$ to ${}^{I}\mathcal{B}$ leads to an additive decomposition of the strain tensor [12]:

$$\begin{gathered}{}^{I}_{\mathrm{A}}\boldsymbol{\varepsilon} = \boldsymbol{F}_e^T \cdot {}_{\mathrm{A}}\boldsymbol{\varepsilon} \cdot \boldsymbol{F}_e = \frac{1}{2}\left(\boldsymbol{F}_e^T \cdot \boldsymbol{F}_e - \boldsymbol{F}_p^{-T} \cdot \boldsymbol{F}_p^{-1}\right) \Longrightarrow {}^{I}_{A}\boldsymbol{\varepsilon} = {}^{I}_{A}\boldsymbol{\varepsilon}_e + {}^{I}_{A}\boldsymbol{\varepsilon}_p \\ \text{with } {}^{I}_{A}\boldsymbol{\varepsilon}_e = \frac{1}{2}(\boldsymbol{F}_e^T \cdot \boldsymbol{F}_e - \mathbf{1}) \text{ and } {}^{I}_{A}\boldsymbol{\varepsilon}_p = \frac{1}{2}\left(\mathbf{1} - \boldsymbol{F}_p^{-T} \cdot \boldsymbol{F}_p^{-1}\right)\end{gathered} \tag{3}$$

In addition to the Euler-Almansi strain tensor, the logarithmic strain tensor or Hencky strain tensor (eq. 4) is a common strain measure for modeling plasticity in metal forming [13].

$${}_{\mathrm{H}}\boldsymbol{\varepsilon} = \frac{1}{2}\ln(\boldsymbol{F}^T \cdot \boldsymbol{F}) = \ln(\boldsymbol{V}) \tag{4}$$

A simple way to show the possibility of additive decomposition for the Hencky strain tensor is to compare its Taylor series (eq. 6) with the Taylor series of the Euler-Almansi strain tensor (eq. 5) around $\mathbf{1}$ respectively. It is obvious that for small strains the terms of higher order can be neglected. Then, the Taylor series of Euler-Almansi and Hencky strain tensors are equivalent. Hence, the Hencky strain tensor can be used for gauging small Euler-Almansi strains.

$$T\left(\frac{1}{2}(\mathbf{1} - \boldsymbol{V}^{-2}); \mathbf{1}\right) = (\boldsymbol{V} - \mathbf{1}) - \frac{3}{2}(\boldsymbol{V} - \mathbf{1})^2 + 2(\boldsymbol{V} - \mathbf{1})^3 - \cdots \tag{5}$$

$$T(\ln(\boldsymbol{V}); \mathbf{1}) = (\boldsymbol{V} - \mathbf{1}) - \frac{1}{2}(\boldsymbol{V} - \mathbf{1})^2 + \frac{1}{3}(\boldsymbol{V} - \mathbf{1})^3 - \cdots \text{ for } |\boldsymbol{V} - \mathbf{1}| < \mathbf{1} \tag{6}$$

In metal forming elastic strains can be considered as small strains. Consequently, the elastic Euler-Almansi strain tensor can be represented by the elastic Hencky strain tensor (${}^{I}_{A}\boldsymbol{\varepsilon}_e \approx {}^{I}_{H}\boldsymbol{\varepsilon}_e$) and the additive decomposition of the Hencky tensor is possible:

$${}^{I}_{H}\boldsymbol{\varepsilon}_p = {}^{I}_{H}\boldsymbol{\varepsilon} - {}^{I}_{H}\boldsymbol{\varepsilon}_e \tag{7}$$

Small elastic strains also allow to model metal elasticity as a linear-elastic isotropic solid, also known as Hooke solid. This elastic constitutive tensor maps the linearized elastic strain tensor (eq. 8) to the Cauchy stress $\boldsymbol{\sigma}$ as described in eq. 9.

$${}_{\mathrm{lin}}\boldsymbol{\varepsilon}_e = \frac{1}{2}(\boldsymbol{F}_e^T + \boldsymbol{F}_e) - \mathbf{1} \tag{8}$$

$$\boldsymbol{\sigma} = \frac{E}{(1+\nu)}\left({}_{\mathrm{lin}}\boldsymbol{\varepsilon}_e + \frac{\nu}{(1-2\nu)}\mathrm{tr}({}_{\mathrm{lin}}\boldsymbol{\varepsilon}_e)\mathbf{1}\right) \tag{9}$$

In eq. 9 E is the Young's modulus and ν is the Poisson's ratio. For homogeneous uniaxial deformations caused by a stress σ_{11}, the uniaxial Hooke law results [11]:

$$\sigma_{11} = E\ {}_{\mathrm{lin}}\varepsilon_{e11} \tag{10}$$

For small strains, different strain measures are almost equal, so it holds:

$$\sigma_{11} = E\ {}^{I}_{H}\varepsilon_{e11} \Longrightarrow \sigma =: E\ {}^{I}_{H}\varepsilon_e \tag{11}$$

In addition, using Cauchy stress is appropriate, because it is work conjugate for both Euler-Almansi and Hencky strain measures [14]. Eq. 11 shows the possibility to determine a strain dependent elastic modulus consistently using a cyclic uniaxial tensile test. Based on the force F and longitudinal

displacement l, the Cauchy stress σ is calculated as the force divided by the actual cross sectional area perpendicular to the force vector. Constant volume is assumed for the whole test (eq. 12). In chapter 3.2, the error that occurs due to this assumption is examined more closely.

$$\frac{\mathrm{d}V}{\mathrm{d}^0V} = \det(\boldsymbol{F}) = 1 \implies \sigma = \frac{F}{A} = \frac{1}{\det(\boldsymbol{F})}\frac{F}{^0A}\frac{l}{^0l} = \frac{F}{^0A}\frac{l}{^0l} \tag{12}$$

For the uniaxial tensile test the total Hencky strains are calculated as follows:

$$_H\varepsilon_e = \ln\left(\frac{l}{^0l}\right) \tag{13}$$

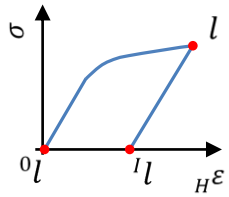

Figure 2. Schematic explanation for l.

Finally, Young's modulus is determined according to (compare fig. 2):

$$E(l) = \frac{\sigma}{_H^l\varepsilon_e} = \frac{F}{^0A}\frac{l}{^0l}\frac{1}{\ln\left(\frac{l}{^Tl}\right)} \tag{14}$$

By conducting cyclic loadings at various prestrains, it is possible to calculate a strain dependent Young's modulus $E(_H\varepsilon)$. Therewith, it is possible to determine a flow curve $\sigma(_H\varepsilon_p)$ using the consistent additive decomposition of Hencky strains:

$$_H\varepsilon_p = {}_H\varepsilon - \frac{\sigma}{E(_H\varepsilon)} \tag{15}$$

3. Determination of Young's modulus

The recommendation for the determination of an initial Young's modulus utilizing an uniaxial tensile test is defined in the standard DIN EN ISO 6892-1:2017-02 [15]. In an iterative process a line of best fit of engineering strain and stress in the elastic domain has to be calculated numerically and visually revised. Due to the small amount of elastic strains, it is feasible to use engineering strain and stress, because differences between different strain and stress measures are negligible. The slope of the best fit line is used as Young's modulus. Former studies showed, that lower and upper borders of the line of best fit are crucial for the calculation of Young's moduli, because of the mentioned nonlinear elastic behavior. Young's moduli differ widely depending on the determination method [16]. In the standard borders depending on $R_{p0.2}$ are suggested. However, to determine $R_{p0.2}$, Young's modulus is necessary, which obviously leads to a conflict [16]. Thus, different determination methods are described in the following.

3.1. Methods for Young's modulus determination

In each cycle, loading and unloading data are split by the point of maximum strain. Young's modulus determination with fixed lower and upper borders is described in Sonne [16]. As already mentioned, it is not expedient to have borders depending on $R_{p0.2}$, hence the borders are defined according to the tensile strength (*TS*). For the method called 'Simple Fit' (Sim.) within this study, the lower border is defined as 0.05, the upper border as 0.18 times *TS* in case of loading. In case of unloading, Yoshida et al. [10] proposed to divide the unloading curve into four sections depending on the stress before unloading σ_*: Yosh. 1: $0.75\sigma_* \leq \sigma \leq 0.95\sigma_*$; Yosh. 2: $0.50\sigma_* \leq \sigma \leq 0.95\sigma_*$; Yosh. 3: $0.25\sigma_* \leq \sigma \leq 0.95\sigma_*$; Yosh. 4: $0 \leq \sigma \leq 0.95\sigma_*$. Young's modulus is the average slope of each section. The comparison of the resulting Young's moduli clarifies the effect of using different borders. Furthermore, a dynamic regression, called 'Regression' (Reg.) within this study, is applied. Starting from zero stress, a regression line is calculated with the first 21 measurement points. Afterwards the area of 21 points is expanded step by step until 0.7 times *TS*. Furthermore, the starting point for the dynamic regression moves along the measurement data. For each area lines of best fits are calculated and the slope obtaining the least squared errors, is stored. Young's modulus is identified as the maximum value of all stored slopes. The method 'Secant' (Sec.) fits a line through the points of intersections of the hysteresis and its slope is taken as Young's modulus.

3.2. Examination of the approach of constant volume

For the evaluations of this study, constant volume is assumed during the whole test, but in fact, lateral contraction changes during elastic and plastic deformation. Hence, by taking constant volume for the

whole test, an error occurs. To examine this error, the specimen were strained up to three different prestrains (3 %, 6 % and 9 % engineering strain) and unloaded afterwards. The cross sectional area of the specimen was measured manually before the test, before and after unloading. These measured cross sectional areas were compared to the corresponding cross sectional areas calculated using the assumption of constant volume. The percent error between experimental data and calculated values is 0.025 % for 3 %, 0.042 % for 6 % and 0.069 % for 9 % prestrain. The accuracy is assumed to be adequate to use the assumption of constant volume for the calculation of Cauchy stress.

4. Experimental Method

Cyclic tensile tests were performed. For the tensile test a standard tensile testing machine is used. The specimen is clamped with a hydraulic clamping system and the strain is tactually measured directly on the specimen. Every cross sectional area is manually measured before the test. For the tests flat specimen of the mild steel DX56 with a thickness of 1.5 mm were used. The initial length ${}^0l$ is 50 mm. The specimen were unloaded and reloaded every 1.5 % engineering strain with a position-controlled speed of 0.048 mm/min. Each cycle until uniform elongation is considered for the evaluation. To ensure that cyclic loading and unloading has no influence on the materials' flow curve, standard tensile tests were performed, too. The specimens were strained until 3 %, 6 % and 9 % engineering strain respectively and unloaded subsequently. These curves were compared to the cyclic tensile test curves and no significant deviation of hardening behavior was noticed.

5. Results

To examine the approach, which was derived in chapter 2, fig. 3 shows the comparison of Young's modulus' behavior for Euler-Almansi and Hencky strain measures. Young's modulus is calculated using 'Regression' for loading and unloading as well as 'Secant' for corresponding hysteresis. The differences between Young's moduli are negligibly and thus the approach is expedient.

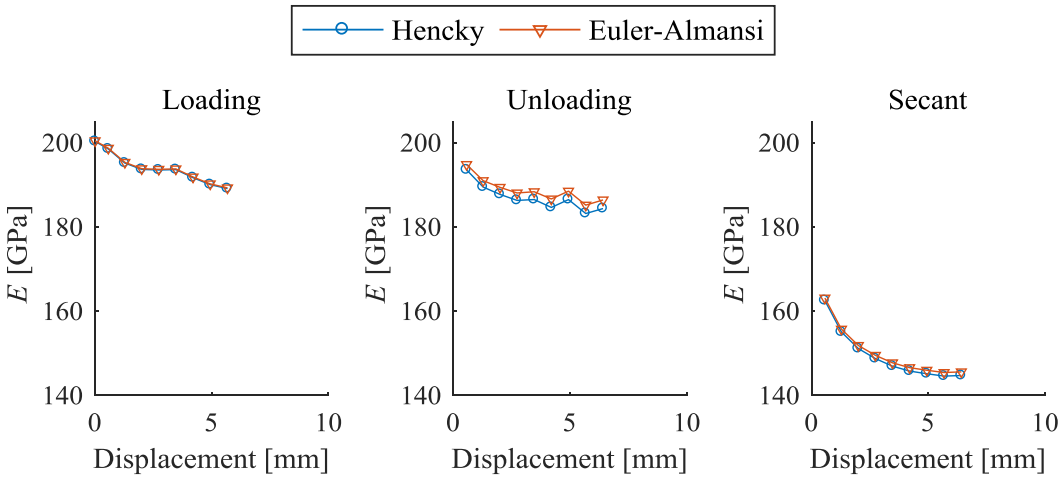

Figure 3. Comparison of the influence of Hencky and Euler-Almansi strain on Young's modulus.

Fig. 4 shows the resulting Young's moduli of the cyclic tensile tests. For the determination of the loading moduli, the methods 'Simple Fit' and 'Regression' were used. With a determined initial Young's modulus of 201 GPa, the method 'Regression' is in good agreement with the common value for steel 210 GPa. Young's moduli determined by 'Simple Fit' are about 7 GPa lower. For both methods the loading Young's modulus decreases by around 5 % until uniform elongation.
The unloading Young's moduli were determined with the methods 'Regression', 'Secant' and 'Yoshida 1 - 4' for each cycle (chapter 3.1). The initial Young's modulus varies by about 35 GPa depending on the determination method. All methods show a strain dependent decrease of the unloading Young's modulus between 5 % ('Regression') and 12 % ('Yosh. 4').

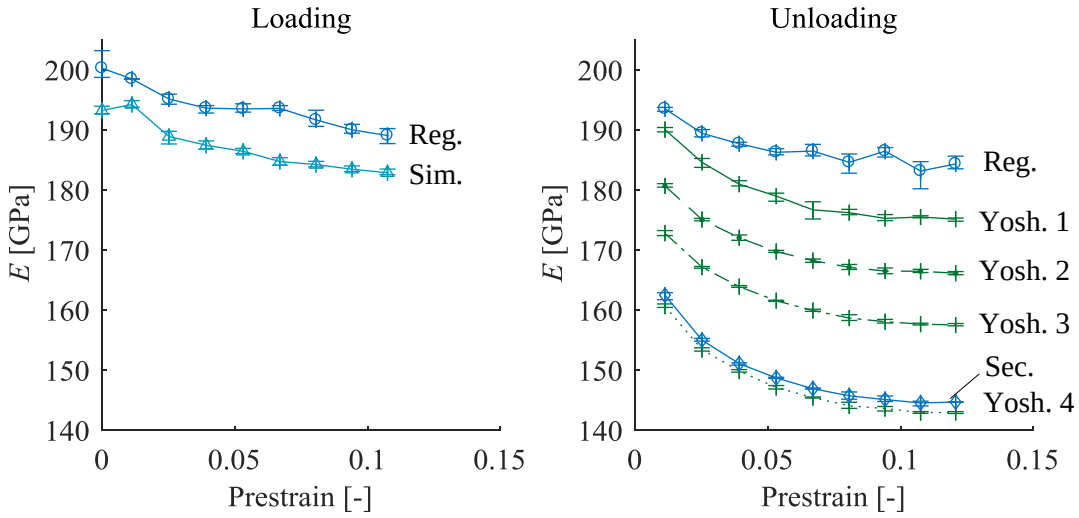

Figure 4. Strain dependency of Young's modulus for loading and unloading. Comparison of different evaluation methods.

It is obvious, that the determination method strongly influences Young's modulus. The calculation of flow curve and springback is in turn influenced by Young's modulus and hence the effect of different values for Young's modulus are investigated. Fig. 5a shows the experimental (Exp.) unloading curve at 0.094 Hencky prestrain in comparison to the unloading behavior derived from the different Young's moduli. At zero Cauchy stress the maximum deviation occurs between Yosh. 4 and the initial Young's modulus (Ini.). This deviation of $7 \cdot 10^{-4}$ elastic recovery strain is small compared to the total strain and thus has no significant influence on the flow curve. However, for an accurate prediction of springback it is crucial to model the unloading curve appropriately. Because the calculation of Young's modulus significantly depends on the determination method, an insensitive approach would enhance springback

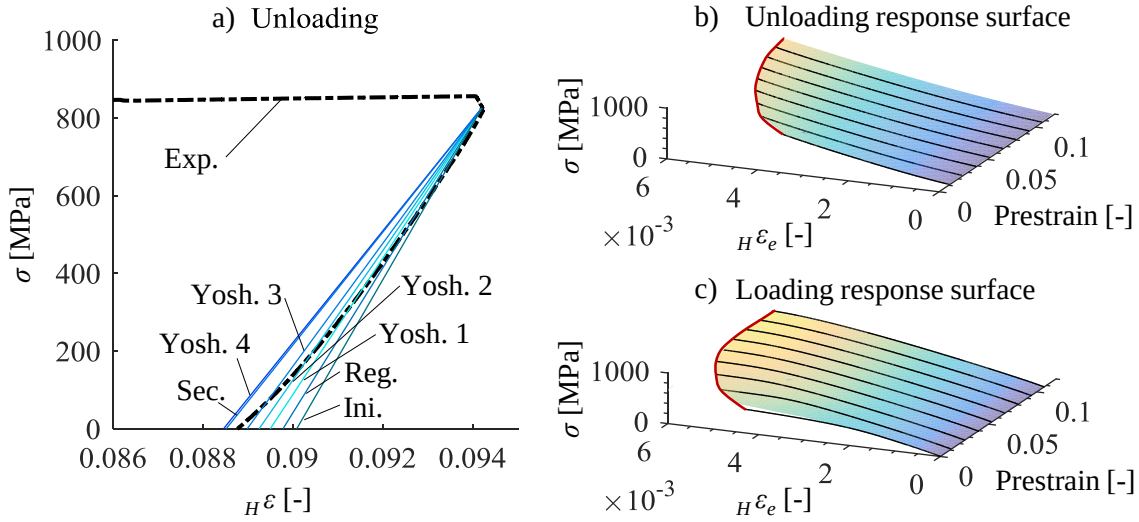

Figure 5. a) Illustration of evaluation methods in comparison with experimental unloading curve. Response surface for unloading (b) and loading (c) elastic recovery strain.

calculation. That is why a three dimensional table of Cauchy stress, prestrain and elastic strain is proposed for predicting arbitrary unloading.

Fig. 5b shows the 'Unloading response surface' based on the cyclic tensile test data. A response surface for loading can be established analogously in case of complete unloading (fig. 5c). The black lines represent the unloading curves of the particular cycles. By implementing the response surface in a FE analysis software, elastic recovery strain for arbitrary stresses and prestrains can be obtained, without assuming linear elastic unloading behavior. A cyclic tensile test of at least one loading and unloading is required for this method merely.

6. Conclusion and Outlook

Under the assumption of small elastic strains the additive decomposition of Euler-Almansi was adopted for Hencky strain and validated using cyclic tensile tests. The strain dependency of Young's modulus was shown a different determination methods were applied and compared. It was noted, that Young's modulus is varying significantly depending on the method. For an accurate springback prediction, a data-based approach is proposed, which allows a precise prediction of the elastic recovery strain in numerical analysis. Further investigations of the nonlinear elastic unloading behavior are necessary to improve springback analysis. An investigation of a strain dependent lateral contraction in comparison to the assumption of constant volume, especially in the region of elastic plastic transition, should be focused. Furthermore, microscopic analysis are essential to investigate and prove macroscopic conjectures and explanations of the material behavior.

Acknowledgement

The authors would like to thank the German Research Foundation (DFG) for the financial support under the grant number VO 1487/27 and VO 1487/28.

References

[1] Banabic D 2010 *Sheet metal forming processes: Constitutive modelling and numerical simulation*
[2] Roll K, Lemke T and Wiegand K 2005 Possibilities and Strategies for Simulations and Compensation for Springback *American Inst. of Phys.*
[3] Roll K, Lemke T and Wiegand K (eds) 2004 Simulationsgestützte Kompensation der Rückfederung *LS-DYNA Anwenderforum (Bamberg)*
[4] Siegert K 2015 *Blechumformung: Verfahren, werkzeuge und maschinen (VDI)*
[5] Morestin F and Boivin M 1996 On the necessity of taking into account the variation in the Young modulus with plastic strain in elastic-plastic software *Nucl. Eng. and Design* 107–16
[6] Andar M O, Kuwabara T, Yonemura S and Uenishi A 2010 Elastic–Plastic and Inelastic Characteristics of High Strength Steel Sheets under Biaxial Loading and Unloading *ISIJ Int.* **Vol.50** 613–9
[7] Cleveland R M and Ghosh A K 2002 Inelastic effects on springback in metals *Int. J. Plast.* **18** 769–85
[8] Doege E, Kulp S and Sunderkötter C 2002 Properties and application of TRIP-steel in sheet metal forming *Steel research* **73** 303–8
[9] Luo L and Ghosh A K 2003 Elastic and Inelastic Recovery After Plastic Deformation of DQSK Steel Sheet *J. Eng. Mater. Technol.* **125** 237
[10] Yoshida F, Uemori T and Fujiwara K 2002 Elastic–plastic behavior of steel sheets under in-plane cyclic tension–compression at large strain *Int. J. Plast.* **18** 633–59
[11] Haupt P 2002 *Continuum Mechanics and Theory of Materials* (Berlin, Heidelberg: Springer)
[12] Volk W 1999 Untersuchung des Lokalisierungsverhaltens mikropolarer poröser Medien mit Hilfe der Cosserat-Theorie *Dissertation* Inst. of. Mech., Universität Stuttgart
[13] Xiao H, Bruhns O T and Meyers A 1997 Logarithmic strain, logarithmic spin and logarithmic rate *A. Mech.* **124** 89–105
[14] Macvean D B 1968 Die Elementararbeit in einem Kontinuum und die Zuordnung von Spannungs- und Verzerrungstensoren *J. of Appl. Math. and Phys. (ZAMP)* **19** 157–85
[15] Deutsches Institut für Normung e.V. 2017 Metallische Werkstoffe – Zugversuch – Teil 1: Prüfverfahren bei Raumtemperatur (ISO 6892-1:2016); (Berlin: Beuth Verlag GmbH)
[16] Sonne H M 1999 Bestimmung des Elastizitäsmoduls im Zugversuch*, Bad Nauheim* 219–30